

# Original Digital Color Image Reconstruction Using Smooth Hue Transition Estimation Method

<sup>1</sup>Prabhakar Rao B, <sup>2</sup>Shraddha Prasad, <sup>3</sup>B.P.Pradeep kumar

**Abstract---** *The reconstruction of digital color image nearer to its originality using non-adaptive estimation methods will produce zipper-effects or artifacts in general. But though the smooth hue transition color estimation method is also non-adaptive, it overcomes the problem of the artifacts and reconstructs the original image in a better way. The color estimation methods are mathematically analyzed and implemented using Matrix Laboratory tool for the digital image is not an image for an engineer but a matrix of numbers from zero through two hundred and fifty-five. As a result of implementation, images and Minimum Mean Square Errors and Signal to Noise Ratios are obtained. The performance evaluation of the algorithms under consideration is done with their help. These digital color image reconstruction methods are widely used for commercial, educational and entertainment, machine and robotic vision applications. These are cost-effective color image reconstruction methods due to the usage of single chip charge couple device for capturing primary colors of the original scene.*

**Keyword---** *Digital Color Image Reconstruction, Smooth Hue, Performance metrics.*

## I INTRODUCTION

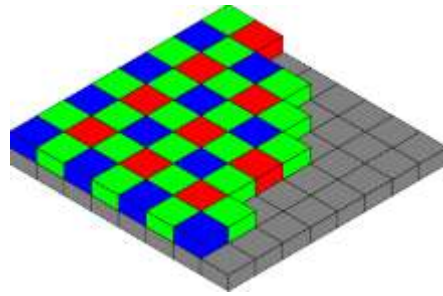
The 2009 Noble Prize winning invention of charge coupled device (CCD) in 1969 by W.S. Boyle and G.E. Smith revolutionized the way images are captured, stored, processed and transmitted [1]. During an image capture process, a digital camera performs various processing mechanisms of the imaging pipeline, an important component of it is colour filter array (CFA) interpolation i.e., to recover a full-resolution image from its CFA data.

To produce a colour image, there should be at least three colour samples at each pixel location. A more cost-effective and relatively less complex solution is to put a CFA in front of the sensor to capture one colour component at a pixel and then interpolate the missing two colour components. Among many CFA patterns, the most commonly used is the Bayer pattern [2]. The Bayer CFA array is shown in Fig.1.

1, Dept. of EEE, Jharkhand Rai University Ranchi, , Jharkhand, India.

2, Faculty of Science and Engineering, Jharkhand Rai University Ranchi, Jharkhand, India

3, Faculty of Electronics and Communication Engineering, Hkbkce, Bangalore, India



**Bayer Pattern of Color Filter Array**

Here the Green filters are in quincunx (interlaced) grid with Red, Blue filters fill up the empty locations. As shown in Fig. 2, the rest of the sensor array is determined by the repeating this pattern both horizontally and vertically, R. Kimmel [3]. Here 50% of Green 25% of Red and 25% of Blue pixels of the original image will be available after sub sampling the datasets. The green channel is measured at a higher sampling rate than the other two because the peak sensitivity of the human visual system (HVS) lies in the medium wavelengths, corresponding to the green portion of the spectrum, D. Alleysson, S. Susstrunk and J. Herault [4]. Although we limit our discussion to the interpolation problem with reference to the Bayer pattern here, the interpolation methods developed for Bayer pattern can in general be extended to other patterns. Because of the mosaic pattern of the CFA, this interpolation process has been widely known as “demosaicing”. Systematic analysis and comparison of different CFA patterns are referred to recent works.

## II LITERATURE REVIEW

The presence of CFA between lens and sensor produces ‘mosaic’ of color samples. The mosaic of colors needs to be undone to recover three color planes in order to obtain a full color representation of the scene information. This process interpolating the missing color sample is referred to as demosaicking, Ngai Li, Jim S. Jimmy Li, and Sharmil Randhawa [5]. There are a variety of methods available for this interpolation process [6]- [7].

Interpolation Methods for Digital Color Image Reconstruction are classified as Non -adaptive algorithms and Adaptive algorithms. 1. Nearest Neighbor Replication (NNR) also called as Closest Neighborhood Interpolation Algorithm (CNA), 2. Bilinear Interpolation (BILIN), 3. Median Interpolation (MIA), and 4. Smooth Hue Transition Interpolation (SHTIA) belong to non-adaptive color estimation methods category. These are the non-adaptive color estimation methods studied, analyzed and implemented. Then their performance is evaluated at subjective and objective levels in this research article.

### Non -adaptive color estimation methods

1) *Nearest Neighbor Replication (NNR) Method:* It is also called as Closest Neighborhood interpolation algorithms (CNA). It’s a simplest method.

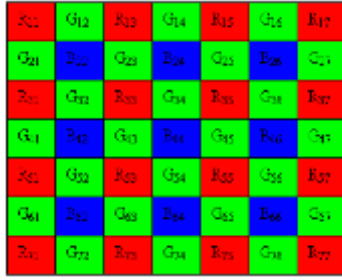


Fig. 1. Bayer CFA Pattern for Interpolation Procedure

It assigns a color value with the nearest known red, green or blue pixel value in the same color plane. There is usually some ordering as to which (left, right, top, or below) nearest neighbor to use for the particular implementation, Ozawa.N [8]. However, it does not do a good job of interpolation, and it creates zigzag zipper color artifacts that distort the image.

**Bilinear Interpolation (BILIN) Method:**

This is another Simplest and little faster method of interpolation algorithms. The bilinear interpolation allocates the missing color component with the linear average of the adjacent pixels with same color component, Hamilton and Adams [9]. For example, the pixel location (2,2) in Fig. 2 contains blue component only. Hence the missing green component can be estimated as average of the left, right, top and bottom green pixel values. The missing red component can be estimated as average of the four diagonally adjacent corner neighbors containing red pixels. Arabic Numbers are used to represent rows and columns of green, red and blue colors. Bilinear Interpolation Process is given in steps below from (1.1) to (1.3).

**CONTROL SCHEME** Interpolation of Green Pixel  $G_{22}$  in position Blue Pixel  $B_{22}$  is given by

$$G_{22} = \frac{G_{12} + G_{32} + G_{21} + G_{23}}{4} \quad (0.1)$$

Interpolation of Blue Pixel  $B_{22}$  in position Blue Pixel  $B_{22}$  is given by

$$B_{22} = B_{22} \quad (0.2)$$

Interpolation of Red pixel  $R_{22}$  in the position of Blue Pixel  $B_{22}$  is given by

$$R_{22} = \frac{R_{11} + R_{33} + R_{31} + R_{13}}{4} \quad (0.3)$$

Similar Procedure can be followed for interpolating other missing pixels.

**Median Interpolation(MIA) Method:** If median interpolation is used at  $B_{22}$  for interpolating missing color samples  $G_{22}$  and  $R_{22}$ , it allocates the missing color component with the “median” value of the adjacent pixels of same color component, as opposed to the linear average used in bilinear interpolation. This provides a slightly better result in terms of visual quality as compared with the bilinear interpolation. However, the resultant images are still blurry

for images with high frequency contents, and for high resolution still imaging system, this is still not acceptable. Median Interpolation Process is given in steps below from (1.4) to (1.6). T. W. Freeman [10].

The Chrominance  $B_{22}$  at  $B_{22}$  is available

$$B_{22} = B_{22} \quad (0.4)$$

To find the Chrominance  $R_{22}$  of the Bayer pattern at  $B_{22}$ , we have to calculate the median of the neighbour pixels  $R_{22}$

$$R_{22} = \text{Median}(R_{11}, R_{13}, R_{31}, R_{33}) \quad (0.5)$$

To find the missing Luminance pixel lines  $G_{22}$  at  $B_{22}$ , the median of the neighboring pixels of  $G_{22}$  is to be calculated

$$G_{22} = \text{Median}(G_{21}, G_{23}, G_{12}, G_{32}) \quad (0.6)$$

Smooth Hue Transition Interpolation ( SHTIA ) Method: The key problem of the color artifacts in both bilinear and median interpolation is that the hue values of adjacent pixels change suddenly (non-smoothly). On the other hand, the Bayer CFA pattern can be considered as combination of a luminance channel (green pixels) and two chrominance channels (red and blue pixels). The smooth hue transition interpolation method interpolates these channels differently, David.R.Cok [11]. The missing green component in every red and blue pixel locations in the Bayer pattern can first be interpolated using bilinear interpolation as discussed before. The idea of chrominance channel interpolation is to impose a smooth transition in hue value from pixel to pixel. In order to do so, it defines blue "hue value" as  $B/G$ , and red "hue value" as  $R/G$ . For interpolation of the missing blue pixel values  $B$ , in pixel location  $(m, n)$  in the Bayer pattern, the following three different cases may arise, as given in steps below from (1.7) to (1.9).

**As shown in pixel location in (2,3) Fig.2, If the pixel location  $(m, n)$  contains Green color component only and the adjacent left and right pixel locations contain Blue color component only, then the Blue information in location  $(m, n)$  can be estimated as follows:**

$$B(m, n) = G(m, n) \times \frac{1}{2} \times \left\{ \left( \frac{B(m, n-1)}{G(m, n-1)} \right) + \left( \frac{B(m, n+1)}{G(m, n+1)} \right) \right\} \quad (0.7)$$

**As shown in pixel location (3,2) in Fig.2, If the pixel location  $(m,n)$  contains Green color component only and the adjacent top and bottom pixel locations contain Blue color component only, then the Blue information in the location  $(m,n)$  can be estimated as follows:**

$$B(m, n) = G(m, n) \times \frac{1}{2} \times \left\{ \left( \frac{B(m-1, n)}{G(m-1, n)} \right) + \left( \frac{B(m+1, n)}{G(m+1, n)} \right) \right\} \quad (0.8)$$

**As shown in pixel location (3,3) in Fig.2.; If the pixel location (m, n) contains Red color component only. Obviously, four diagonally neighboring corner pixels contain Blue color only, Then BLUE information in location (m, n) can be estimated as follows:**

$$B(m,n) = G(m,n) \times \frac{1}{4} \times \left\{ \begin{array}{l} \left( \frac{B(m-1,n-1)}{G(m-1,n-1)} \right) \\ + \left( \frac{B(m-1,n+1)}{G(m-1,n+1)} \right) \\ + \left( \frac{B(m+1,n-1)}{G(m+1,n-1)} \right) \\ + \left( \frac{B(m+1,n+1)}{G(m+1,n+1)} \right) \end{array} \right\} \quad (0.9)$$

The interpolation of missing *Red* pixel values can be carried out similarly. Depending on the location, interpolation step happens, and the definition of "hue value" changes. For example, if the pixel value is transformed into logarithmic exposure space from linear space before interpolation, instead of  $B/G$  or  $R/G$ , one can now define the "hue value" as  $(B-G)$  or  $(R-G)$ . This is coming from the fact that  $\log(X/Y) = \log(X) - \log(Y) = X' - Y'$ . Here  $X'$  and  $Y'$  are the logarithmic values of  $X$  and  $Y$  respectively. Since the linear/nonlinear transformation can be done using a simple table look-up and all the division for calculating hue value is replaced by subtraction, this helps reduce computational complexity for implementation. The adaptive color estimation and image reconstruction methods do exist in the literature [12], [13] but the concentration in this research paper is to analyze, implement and establish that non-adaptive and less complex algorithms also can be used to reduce the artifacts and zipper effects.

### III PERFORMANCE EVALUATION

The evaluation of performance of Interpolation methods is done at two levels i.e., Subjective and Objective levels. Wenmain Lu and Yap-peng Tan [14].

#### Subjective Performance Evaluation

Fig. 3 shows from top to bottom the original image, 2D and 3D Bayer arrays of the test image 1 i.e., image of Macaws, a standard test image taken from the Kodak test image data base. Fig. 4 shows from top to bottom the original image, 2D and 3D Bayer patterns of test image 2 i.e., image of St. Mary's Engineering College, Hyderabad. Fig. 5 to Fig. 8 show the resultant images of test image1 obtained using Interpolation methods 1 to 4. Fig. 9 to Fig. 12 show the resultant images of test image 2 implemented for Interpolation methods 1 to 4. MATLAB is used for implementation. From Fig. 3 to Fig. 12 are presented here for the evaluation of the interpolation methods at subjective level. The viewer can observe and interpret the results for the performance of the algorithms but this method is not a perfect one. Hence Objective Performance evaluation is necessary.



**Fig. 3: Original image, 2D and 3D Bayer Array of Test Image**



**Fig. 4: Original image, 2D and 3D Bayer Array of Test Image 2**



**Fig. 5: Resultant Image of test image 1 for interpolation method 1**



**Fig. 6: Resultant Image of test image 1 for interpolation method 2**



**Fig. 7: Resultant Image of test image 1 for interpolation method 3**



**Fig. 8: Resultant Image of test image 1 for interpolation method 4**



**Fig. 9: Resultant Image of test image 2 for interpolation method 1**



**Fig. 10: Resultant Image of test image 2 for interpolation method 2**



**Fig. 11: Resultant Image of test image 2 for interpolation method 3**



**Fig. 12: Resultant Image of test image 2 for interpolation method 4**

### **Objective Performance Evaluation**

The Objective Performance metrics used here to evaluate the performance of the interpolation methods are Minimum Mean Square Error (MMSE) and Signal to Noise Ratio (SNR) obtained through the implementation of the algorithms for test images 1 and 2 using MATLAB.

#### **Minimum Mean Square Error (MMSE)**

MMSE corresponds to the expected value of the squared error loss or quadratic loss. It measures the average of the squared error. Minimum is its value, better is the performance of the interpolation method.

$$MMSE = \frac{\sum_{x=1}^m \sum_{y=1}^n [I_o(x, y) - I_r(x, y)]^2}{(m \times n)} \quad (0.10)$$

Where (m×n): size of the image,  $I_o(x, y)$ : Original Image,  $I_r(x, y)$ : Reconstructed Image.

#### **Signal to Noise Ratio(SNR)**

SNR is a measure used to quantify how much a signal has been corrupted by the unwanted signal. It is defined as the ratio of signal power to the noise power corrupting the signal.

$$SNR = \left[ -10 \log \right] \frac{\frac{1}{KL} \sum_{k=1}^{K-1} \sum_{l=1}^{L-1} (I_o(k, l) - I_r(k, l))^2}{255^2} [dB] \quad (0.11)$$

Where the product KL: Spatial Resolution of the image; the numerator represents the squared average pixel value of the image; and the denominator represents the squared color resolution.

The objective performance metrics MMSE and SNR values obtained using Interpolation Methods 1 to 4 (CNA/NNA, MIA, BILIN, and SHITA) for test image 1 and 2 respectively are Tabulated in TABLE I to TABLE IV.

For interpretation of results obtained after implementing algorithms 1 to 4, bar charts of MMSE and SNR values of Test images 1 and 2 are depicted from Fig. 13 to Fig. 16.



**Table 1: objective performance metrics-mmse of test image 1**

S.No.	Interpolation Method	Minimum Mean Square Error		
		Red	Green	Blue
1	CNA/NNA	6.9342	4.3953	7.1951
2	MIA	3.6307	2.3016	3.7778
3	BILIN	3.4694	2.3193	3.5620
4	SHITA	3.8672	2.3463	2.5114

**Table 2: objective performance metrics- snr of test image 1**

S.No.	Interpolation method	signal to noise ratio		
		red	Green	Blue
1	CNA/NNA	43.6874	45.6535	43.5272
2	MIA	46.1088	49.2817	45.9656
3	BILIN	46.4683	49.2485	46.3652
4	SHITA	45.9152	49.1982	47.5434

**Table 3: objective performance metrics- MMSE of test image 2**

S.No.	Interpolation Method	Minimum Mean Square Error		
		RED	GREEN	BLUE
1	CNA/NNA	34.1288	26.7500	35.8306
2	MIA	31.8643	21.0043	33.0435
3	BILIN	32.9541	24.4220	33.5819
4	SHITA	33.0005	24.5569	34.7842

**Table 4: objective performance metrics- SNR of test image 2**

S.No.	Interpolation Method	Signal to Noise Ratio		
		Red	Green	Blue
1	CAN/NNA	36.0550	37.7186	41.2688
2	MIA	36.5409	38.7566	36.4215
3	BILIN	36.4251	38.1801	36.3667
4	SHITA	36.2688	38.1603	36.0885

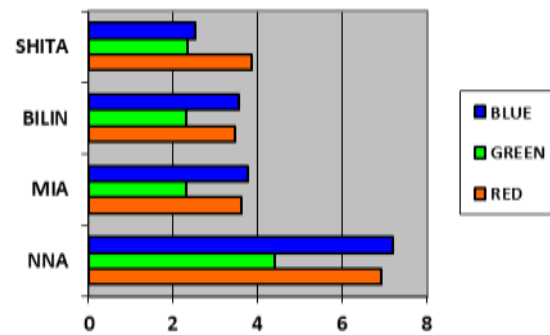


**Fig. 13: Bar chart of MMSE values of test image 1 for interpolation methods 1 to 4**

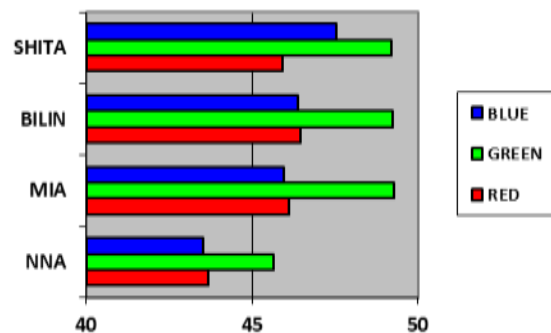


**Fig. 14: Bar chart of SNR values of test image 1 for interpolation methods 1 to 4**

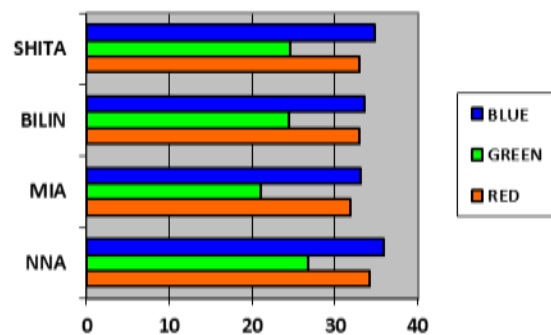


**Fig. 15: Bar chart of MMSE values of test image 2 for interpolation methods 1 to 4**

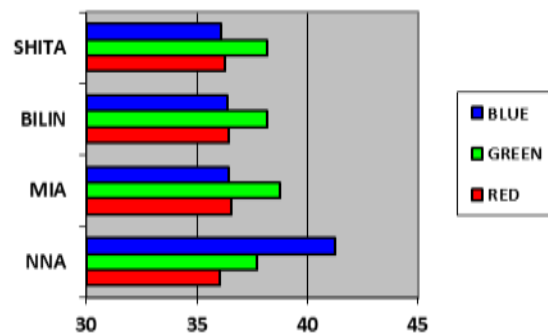


**Fig. 16: Bar chart of SNR values of test image 2 for interpolation methods 1 to 4**

#### IV INTERPRETATION OF THE RESULTS

The resultant images presented in Fig. 3 to 12 will help the viewer in evaluating subjectively the performance of the interpolation methods. But all images look alike to a naked eye. Hence the Objective performance metrics MMSE and SNR will help anyone to evaluate objectively. Minimum is the value of MMSE; and greater is the value of SNR, better is the performance of the algorithm. From the graphic charts of MMSE and SNR shown in Fig. 13 to Fig.16; and from observing Table I to Table IV, it is clear that on an average smooth hue transition color estimation method do better compared with other non- adaptive algorithms. Its MMSE is least and SNR is greater relatively. Graph chart of resultant MMSE and SNR values of interpolation methods 1 to 4 for test image 1 and 2.

#### V CONCLUSION

In this paper, four non adaptive color image reconstruction algorithms are implemented using MATLAB, after due theoretical study and mathematical analysis. The comparative performance analysis-subjective and objective quality (MSE& SNR) of reconstructed images is done. For the digital design of machine, robotic or artificial vision devices, if we were to choose one only from the algorithms we have considered here, and then smooth hue transition color estimation can be preferred.

#### VI FUTURE ENHANCEMENTS

The adaptive color estimation and image reconstruction- interpolation methods can be analyzed theoretically and mathematically, implemented using an appropriate tool and can be evaluated based subjective and objective performance evaluation metrics can also be explored and implemented.

#### REFERENCES

- [1] Manoharan, Rajesh, et al. "Selection of Intermediate Routes for Secure Data Communication Systems using Graph Theory Application and Grey Wolf Optimization Algorithm in MANETs." *IET Networks* (2020).
- [2] Rajesh, M., Gnanasekar, J.M. Path Observation Based Physical Routing Protocol for Wireless Ad Hoc Networks. *Wireless Pers Commun* **97**, 1267–1289 (2017). <https://doi.org/10.1007/s11277-017-4565-9>

- [3] Rajesh, M. Streamlining Radio Network Organizing Enlargement Towards Microcellular Frameworks. *Wireless Pers Commun* (2020). <https://doi.org/10.1007/s11277-020-07336-9>
- [4] W.S.Boyle and G.E.Smith, "Information storage devices," U.S.Patent 3,858,232. 1974.
- [5] B.E.Bayer and Eastman Kodak Company, "Color Imaging Array," U.S.Patent 3, 971, 065. 1975
- [6] R.Kimmel, "Demosaicing: image reconstruction from CCD samples," IEEE Trans. Image Process. Vol. 8, No.9, pp.1221–1228, 1999.
- [7] D.Alleysson, S.Susstrunk and J.Herault, "Linear demosaicing inspired by the human visual system," IEEE Transactions on Image Processing, Vol. 14, No. 4, pp. 439-449, April 2005.
- [8] Ngai Li, Jim S. Jimmy Li, and Sharmil Randhawa, "Color Filter Array Demosaicking Based on the Distribution of Directional Color Differences," IEEE Signal Processing Letters, Vol. 24, No. 5, May 2017.
- [9] Kumar, V., Prasad, L., Performance Analysis of three sides concave dimple shape roughened solar air heater, J. sustain. dev. energy water environ. syst., 6(4), pp 631-648, 2018.
- [10] Kumar, V., Prasad, L., Experimental investigation on heat transfer and fluid flow of air flowing under three sides concave dimple roughened duct. International Journal of Mechanical Engineering and Technology (IJMET), Volume 8, Issue 11, November 2017, pp. 1083–1094, Article ID: IJMET\_08\_11\_110.
- [11] C.Raja Rao, Mahesh Boddu and Soumithra Kumar Mandal, "Single Sensor Color Filter Array Interpolation Algorithms," 2<sup>nd</sup> International Conference in India, Information Systems Design and Intelligent Applications, Vol.2, Springer India, pp.295-308, 2015.
- [12] R. Rajeev, E. Wesley, L. Griff and S. Williams, "Demosaicking methods for Bayer color arrays," Journal of Electronic Imaging, Vol. 11, No. 3, pp. 306-315, July 2002.
- [13] N.Ozawa, "Chrominance signal interpolation device for a color camera," U.S.Patent No .4716455. 1987.
- [14] Kumar, V., Nusselt number and friction factor correlations of three sides concave dimple roughened solar air heater, Renewable Energy 135 (2019) 355-377.
- [15] Kumar, V., Prasad, L., Experimental analysis of heat transfer and friction for three sides roughened solar air heater, Annales de Chimie - Science des Matériaux, 75-107, ACSM. Volume 41 – n° 1-2/2017.
- [16] J.F.Hamilton Jr., and J.E.Adams, "Adaptive color plane interpolation in single sensor color electronic camera," U.S.Patent 5,629,734. 1997.
- [17] T. W. Freeman, "Median filter for reconstructing missing color samples," U.S. Patent No. 4,724,395. 1998.
- [18] Cok,David.R. "Signal Processing method and apparatus for producing interpolated chrominance values in a sampled color Imaging signal," U.S.Patent No. 4,642,678. 1987.
- [19] R.H.Hibbard, "Apparatus and method for adaptively interpolating a full color image using luminance gradients," U.S.Patent No. 5,382,976. 1995.
- [20] G.A.Laroch and M.A.Prescott, "Apparatus and method for adaptively interpolating a full color image using chrominance gradients," U.S.Patent No. 5,373,322. 1994.
- [21] Wenmain Lu and Yap-peng Tan, "Color filter array demosaicing: new method and performance measures," IEEE Trans. on Image Proc., vol. 12, no. 10, pp. 1194-1210, Oct. 2003.
- [22] Kumar, V., Prasad, L., Thermal performance investigation of one and three sides concave dimple roughened solar air heaters. International Journal of Mechanical Engineering and Technology (IJMET) Volume 8, Issue 12, December 2017, pp. 31–45, Article ID: IJMET\_08\_12\_004.
- [23] Kumar, V., Prasad, L., Performance prediction of three sides hemispherical dimple roughened solar duct, Instrumentation, Measure, Métrologie, 273-293 I2M. Volume 17 – n° 2/2018.